IEEE Access
Multidisciplinary : Rapid Review : Open Access Journal

Received July 12, 2021, accepted July 22, 2021, date of publication July 26, 2021, date of current version August 2, 2021.

Digital Object Identifier 10.1109/ACCESS.2021.3099906

Over-the-Air Computation Strategy Using Space–Time Line Code for Data Collection by Multiple Unmanned Aerial Vehicles

JINGON JOUNG[1], **(Senior Member, IEEE), AND JIANCUN FAN**[2], **(Senior Member, IEEE)**
[1]School of Electrical and Electronics Engineering, Chung-Ang University, Seoul 06974, South Korea
[2]School of Information and Communications Engineering, Xi'an Jiaotong University, Xi'an 710049, China

Corresponding author: Jingon Joung (jgjoung@cau.ac.kr)

This work was supported in part by the National Research Foundation of Korea (NRF) Grant through the Korean Government (MSIT) under Grant NRF-2019R1A2C1084168 and Grant 2021R1A4A2001316, and in part by the Institute of Information and Communications Technology Planning and Evaluation (IITP) Grant through the Korean Government (MSIT) (Development of Next Generation Wireless Access Technology Based on Space Time Line Code, 50%) under Grant 2021-0-00874.

ABSTRACT In this study, we investigated a data collection system for multiple unmanned aerial vehicles (UAVs) in the sky. To reduce the required data collection time for a time-division multiple access (TDMA)-based protocol, an over-the-air computation (OAC) strategy was employed, and the average values of data computed. In this method, multiple single-antenna sensing UAVs (sUAVs) report the sensing data to a two-antenna data-collection UAV (dUAV) through the OAC strategy. To this end, we propose an efficient OAC strategy using a space-time line code (STLC) scheme that can achieve a full spatial diversity gain. Using the efficient data collection protocol of the proposed STLC-OAC strategy, the overall operation time for data collection can be significantly reduced relative to s TDMA-based strategy. Furthermore, the proposed STLC-OAC strategy can reduce the normalized mean square error (NMSE) of the estimated average value of the data relative to that of the TDMA-based method. As the gap in the NMSEs between TDMA- and STLC-OAC-based strategies was observed to increase as the number of sUAVs increased, it can be concluded that the proposed STLC-OAC strategy is advantageous for UAV-based data collection systems, especially when a large number of sUAVs report the sensing data.

INDEX TERMS Sensors, data collection, over-the-air computation (OAC), space-time line code (STLC), unmanned aerial vehicle (UAV).

I. INTRODUCTION

The rapid and wide growth of the ‘‘internet of things’’ and ‘‘internet of everything’’ has increased the application of sensors in various fields. For example, recently, unmanned aerial vehicles (UAVs) have used considered to effectively collect sensing data from images taken by UAVs [1]–[4] or from sensors deployed over a wide ground area [5]–[9]. Owing to the enormous applications potentials of UAVs, such as in military, civilian-noncommercial, and civilian-commercial applications (see references in [10] therein), data collection from distributed sensing UAVs (sUAVs) in the sky can be considered as an interesting application of sensing data collection. For example, air quality and pollutants can be monitored by UAVs [11]–[13]. The data monitored by the multiple sUAVs are collected at a data fusion center, e.g., a UAV access point, vehicle access point [13], or ground base station (GBS). The sUAVs directly transfer the monitored data to the GBS if the channel quality from the sUAVs to the GBS is sufficient for communication. In certain cases, however, the direct channels between the sUAVs and GBS can be poor, owing to the long distance between the sUAVs and GBS (or obstacles between the sensing area and the GBS); this causes significant path loss, and the signal strength received directly from sUAVs can be insufficient for reliable data collection at the GBS. To resolve this issue, one of the sUAVs can operate as a data-collecting UAV (dUAV) that collects, preprocesses, and transfers the data to the GBS at a location where it can relay the collected and processed data to the GBS. To this end, the dUAV, which is one of the

The associate editor coordinating the review of this manuscript and approving it for publication was Barbara Masini.

sUAVs, moves from the sensing area to the proper location for relaying. Alternatively, a dedicated UAV can be deployed for cooperation.

One simple strategy to collect sensing data from distributed sUAVs is a time-division multiple access (TDMA)-based protocol. The TDMA-based protocol allows each sUAV to sense and report the sensing data to the GBS or dUAV in a predetermined order of sequential time so that interference among the sUAVs can be avoided. Thus, the TDMA-based protocol requires at least K time resources to collect data from K sUAVs. If the dUAV collects the data from the K sUAVs and the collected data must also be reported to the GBS, the additional K-time resources are required. As the collected data are eventually manipulated to extract meaningful information, such as the average or variance of the data, the dUAV can compute the statistical information before the retransmission of data and retransmit it to the GBS to avoid the additional abuse of the K-time resources. By doing this, the dUAV retransmits the manipulated single data to the GBS using a single-time resource. However, K time resources are still required for the data collection from the K sUAVs; this is a fundamental issue of the TDMA-based protocol. Therefore, when considering a large number of sUAVs, the naive TDMA protocol is prohibited, owing to the inefficient management of time resources for the energy-limited UAV systems. As reported in [6]–[8], [14], the time resource is one of the critical resources for the energy-efficient operation of UAVs, as each UAV must consume a significant amount of energy to hover and fly while it communicates in the air. The abuse of the time resources of the energy-limited UAV systems has hindered the UAV-related businesses from being expanded for various applications in the near future.

To prevent the abuse of the time resources in the TDMA-based protocol when the dUAV computes the statistics of the collected data, an efficient strategy called over-the-air computation (OAC) [15]–[23] can be employed in UAV-based data collection systems [13], [24]. In an OAC-based protocol, multiple sUAVs report the sensing data to the dUAV (or GBS) simultaneously using the same frequency band, that is, in a coordinated multi-point transmission [25], [26]. The multiple received signals are merged (added) into a single signal comprising the summation of the sensing data in the air. Thus, if the dUAV tries to detect the individual sensing data one at a time, other signals interfere with the detected signal. However, the OAC estimates the merged data, not the individual data, and computes some statistics of the data, such as the arithmetic mean, weighted sum, geometric mean, polynomial, and Euclidean norm [13] (this is the reason why this strategy is called OAC). Throughout this study, we focus on the computation of the arithmetic mean of sensing data using multiple sUAVs. Many of the existing studies on OAC assume that multiple antennas are employed at the transmitter (i.e., the sUAV in our system model). However, owing to the high signal processing complexity, the power consumption costs, and the size, weight, and power (SWAP) constraints on the UAVs [27], it is quite costly to employ multiple antennas at sUAVs. Therefore, a single antenna is assumed for the sUAVs. Moreover, we relax the SWAP constraints for the dUAV so that two antennas are employed at the dUAV. The conventional OAC strategy is still difficult to employ directly, because sUAVs have a single antenna.

To employ the OAC strategy to compute an arithmetic mean in the considered UAV data collection system, in which multiple single-antenna sUAVs report the sensing data to a two-antenna dUAV through the OAC strategy, we propose an efficient OAC strategy based on the space-time line code (STLC) scheme proposed in [28]–[30]. The STLC transmitter encodes the information symbols by using channel state information (CSI) and transmits them through a single antenna (not necessarily multiple antennas), and a two-antenna STLC receiver at the dUAV can achieve a full spatial-diversity gain by simply combining the received signals without the full CSI [31]. As it exploits the simplicity and full spatial diversity gain of the STLC, the STLC scheme has been extensively applied in various wireless communication systems, such as multiuser or multi-stream multiplexing systems [29], [32]–[36], cooperative communication systems [37]–[39], orthogonal frequency-division multiplexing systems [40], vehicular and UAV systems [14], [41], security-aware systems [42], [43], and antenna selection systems [44]–[46]. Here, the CSI is assumed to be available at the transmitter under the assumption that the uplink and downlink channels are symmetric in a time-division duplex (TDD) mode. Because the CSI is required at the sUAV rather than the dUAV, the required training period for the CSI estimation of the STLC-based OAC (STLC-OAC) systems can be significantly reduced relative to that of a TDMA-based system. Moreover, multiple sUAVs can report the sensing data simultaneously, and the required reporting time can also be reduced. Although additional reporting times are required for the OAC, the overall operation time can be significantly reduced by using the proposed STLC-OAC strategy. Therefore, the operation time of UAV systems can be prolonged, resulting in an increase in UAV-related commercial opportunities. The evident benefit of the operation time reduction aside, the proposed STLC-OAC method provides a better estimation performance than the conventional TDMA-based method; this is verified by comparing the normalized mean-square errors (NMSEs) of the average values of the data as estimated through the TDMA-based and STLC-OAC strategies. One important observation is that the performance improvement increases as the number of sUAVs increases. Therefore, it can be surmised that the proposed STLC-OAC strategy is relevant for UAV-based data collection systems, especially when there are a large number of sUAVs reporting the sensing data. The proposed STLC-OAC strategy between sUAVs and a dUAV (i.e., cooperative communication from sUAVs to a GBS via a dUAV) can also be applied for direct communication between sUAVs and a GBS.

The remainder of this paper is organized as follows. The UAV system and signal models for sensing data

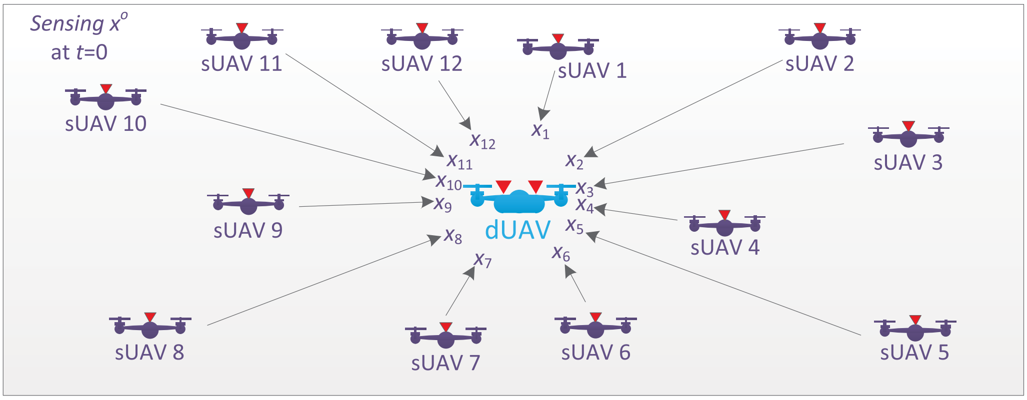

FIGURE 1. Data collection scenario from multiple sUAVs. In this example, 10 sUAVs from sUAV 1 to sUAV 10 are illustrated, i.e., $K = 10$. sUAV k reports the sensing data x_k to a dUAV. The dUAV, with two antennas collects the sensing data x_k from the sUAVs with a single antenna and computes the average value of the sensing data, i.e., E[x_k].

collection are introduced in Section II. In addition, a conventional TDMA-based data-collection strategy is introduced. In Section III, the STLC-OAC strategy is proposed. Section IV presents the verification of the proposed strategy by comparing the NMSE performance with that of the conventional TDMA-based strategy. Finally, Section V concludes the paper.

Notations: The superscripts T, H, $*$, and -1 denote a transposition, Hermitian transposition, complex conjugate, and inversion, respectively, for any scalar, vector, or matrix. The notation $|x|$ denotes the absolute value of x, and $x \sim \mathcal{N}(0, \sigma^2)$ means that a real-value random variable x conforms to a normal distribution with a zero mean and variance σ^2; $x \sim \mathcal{CN}(0, \sigma^2)$ means that a complex random variable x conforms to a complex normal distribution with a zero mean and variance σ^2. E[x] represents the expectation value of the random variable x.

II. SENSING DATA COLLECTION UAV SYSTEM MODEL

As illustrated in Fig. 1, a data collection scenario is considered with K sUAVs and one dUAV, where $K = 10$. Each sUAV has a single antenna, whereas the dUAV has two antennas. The kth sUAV senses a target value denoted by $x^o \in \mathbb{R}^{1\times 1}$, i.e., a ground truth value, and reports it to the dUAV, where $k \in \mathcal{K} = \{1, \ldots, K\}$. The sensing value x_k of sUAV k includes the measurement error v_k, which is modeled as additive white Gaussian noise (AWGN) as follows:

$$x_k = x^o + v_k, \tag{1}$$

where $v_k \sim \mathcal{N}(0, \sigma_v^2)$. The dUAV collects the sensing data from the sUAVs, computes the average of all of the measurements, i.e., $\overline{X} = \mathrm{E}\{x_k\}$, and transmits it to a GBS. As noted above, each sUAV has a single antenna owing to the SWAP limitation, whereas the dUAV has two antennas. However, the results of this study can be readily extended to sUAVs with multiple antennas if the SWAP limitation of the UAVs is resolved. The channel between the sUAV k and dUAV is defined as $\boldsymbol{h}_k = [h_{k,1}, h_{k,2}]^T \in \mathbb{C}^{2\times 1}$, where $h_{k,n}$ is the channel between the antenna of the kth sUAV and nth antenna of the dUAV. For simplicity, the channels are assumed to be independent and identically distributed (i.i.d.) random variables with a $\mathcal{CN}(0, 1)$ distribution, that is Rayleigh fading channels. Notably, the results in this study do not depend on the channel model, and are relevant for different types of channel models, for example, a Rician channel model with a line-of-sight channel, as a single data stream transmission is considered for each sUAV for the given channels.

A. TDMA-BASED STRATEGY

We first introduce a TDMA-based naive method for the dUAV to obtain the average value of the sensing data from the sUAVs. At the kth time, the kth sUAV measures x_k and transmits it to the dUAV. The received signal of the dUAV at time k is expressed as

$$\boldsymbol{y}_k = \boldsymbol{h}_k \mathcal{M}_M \left(\mathcal{Q}_N(x_k)\right) + \boldsymbol{n}_k, \tag{2}$$

where $\mathcal{M}_M(\cdot)$ is a function for modulation with size M with $|\mathcal{M}_M(\cdot)|^2 = P$; $\mathcal{Q}_N(x_k)$ represents the N-bit quantization of x_k, i.e., an analog-to-digital converter, and $\boldsymbol{n}_k \in \mathbb{C}^{2\times 1}$ is an AWGN vector at the dUAV at time k. Here, P is the transmit power of sUAV k, and the transmit power is limited by P for all sUAVs. The variance of the AWGN at each antenna of the dUAV is denoted by σ_n^2 throughout this study. From $\boldsymbol{y}_k$, the dUAV obtains the estimate of x_k as follows:

$$\begin{aligned} \tilde{x}_k &= \mathcal{Q}_N^{-1}\left(\mathcal{M}_M^{-1}\left(\frac{\boldsymbol{h}_k^H}{\|\boldsymbol{h}_k\|^2}\boldsymbol{y}_k\right)\right) && \text{(3a)}\\ &= \mathcal{Q}_N^{-1}\left(\mathcal{M}_M^{-1}\left(\mathcal{M}_M\left(\mathcal{Q}_N(x_k)\right) + \frac{\boldsymbol{h}_k^H\boldsymbol{n}_k}{\|\boldsymbol{h}_k\|^2}\right)\right) && \text{(3b)}\\ &= \mathcal{Q}_N^{-1}\left(\widetilde{\mathcal{Q}_N(x_k)}\right) && \text{(3c)}\\ &\triangleq x_k + e_{k,AWGN} + e_{k,QTZ}, && \text{(3d)} \end{aligned}$$

where $\mathcal{Q}_N^{-1}(\cdot)$ represents the digital-to-analog conversion from N bits to an analog signal, $\mathcal{M}_M^{-1}(\cdot)$ is the demodulation of modulated symbols with size M, and $e_{k,AWGN}$ and $e_{k,QTZ}$ are the error terms caused by the AWGN and quantization, respectively.

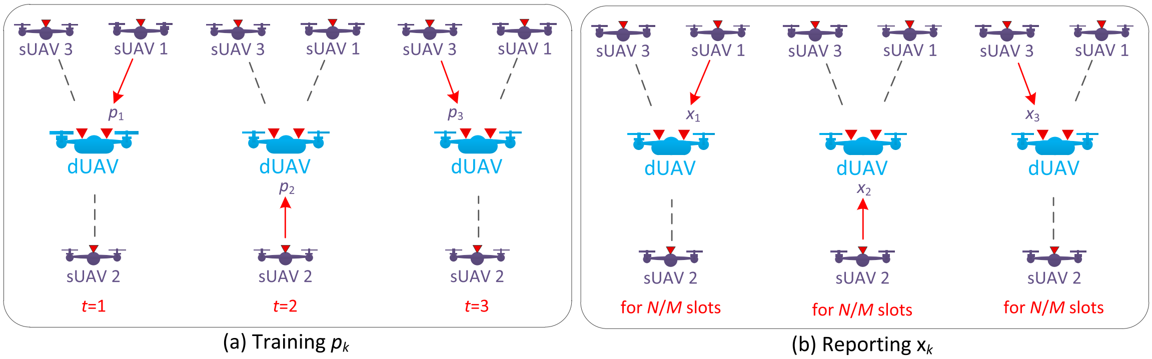

FIGURE 2. TDMA-based sensing data collection scenario with three sUAVs (i.e., $K = 3$). Each sUAV transmits in an orthogonal time slot. (a) Training for estimating CSI at dUAV. (b) Data reporting based on the TDMA strategy.

After all K sUAVs report the data during the K time slots by repeating the same procedures in (2) and (3) for all $k \in \mathcal{K}$ across orthogonal times, i.e., a TDMA procedure, the dUAV can obtain all estimates from all sUAVs and estimate the average value $\overline{X}$ of the estimated sensing data $\tilde{x}$ as follows:

$$\tilde{\overline{X}}_{TDMA} = \frac{1}{K}\sum_{k\in\mathcal{K}}\tilde{x}_k \tag{4a}$$
$$= \frac{1}{K}\sum_{k\in\mathcal{K}}x_k + \frac{1}{K}\sum_{k\in\mathcal{K}}\left(e_{k,AWGN} + e_{k,QTZ}\right) \tag{4b}$$
$$= \overline{X} + e_{TDMA}, \tag{4c}$$

where $\overline{X}$ is the true average value of measurements $\{x_k\}$ that the dUAV intends to estimate, and e_{TDMA} is the estimation error, including the effects from the quantization and AWGN in the TDMA-based data collection method. From (4), the NMSE is defined as a performance metric as follows:

$$\mathrm{NMSE}_{TDMA} = \mathrm{E}\left[\frac{\left|\overline{X} - \tilde{\overline{X}}_{TDMA}\right|^2}{|\overline{X}|^2}\right] = \mathrm{E}\left[\frac{|e_{TDMA}|^2}{|\overline{X}|^2}\right] \leq \frac{\mathrm{E}\,|e_{TDMA}|^2}{\mathrm{E}\,|\overline{X}|^2}, \tag{5}$$

where the expectation is performed for a fixed channel over noise, and the inequality comes from Jensen's inequality.

As described, the estimated average value from the TDMA-based data collection method is distorted by the quantization error and AWGN. Furthermore, one *cycle* of the data report of the TDMA-based method requires the following number of transmission time slots:

$$t_{TDMA} = K\left(\left\lceil\frac{N}{M}\right\rceil + 1\right) \tag{6}$$

for the report from the K sUAVs, each sUAV needs to transmit at least $\lceil\frac{N}{M}\rceil$ information symbols and one pilot symbol. Here, for reliable communications, typically $\lceil\frac{N}{M}\rceil \geq 1$, and thus, $t_{TDMA} \geq 2K$.

For example, at least six time slots are required to estimate the average value of the sensing data from the three sUAVs using the TDMA-based method, as illustrated in Fig. 2. To reduce the quantization error, N can be increased, but this also increases the number of required transmission time slots, t_{TDMA}, for the TDMA. Alternatively, to overcome the AWGN effect, M can be decreased, yet this also increases the time required for the TDMA, i.e., t_{TDMA}. The increase of t_{TDMA} is inefficient and may cause significant latency and discrepancy between the sensing measurement and actual values. Moreover, each sUAV needs to wait for $(K-1)\left(\lceil\frac{N}{M}\rceil+1\right)$ slots until all other $(K-1)$ sUAVs complete their reports, which is also inefficient in terms of energy consumption. As each UAV is a highly energy-limited system, a conventional TDMA-based strategy is irrelevant for UAV-based data collection systems. An OAC strategy can resolve these issues.

B. OAC-BASED STRATEGY

In OAC, all sUAVs transmit data simultaneously, and the received signal at the dUAV is then written as follows:

$$\boldsymbol{y} = \sum_{k\in\mathcal{K}}\boldsymbol{h}_k c x_k + \boldsymbol{n}, \tag{7}$$

where c is a *transmit power normalization factor* for fulfilling the maximum transmit power constraint P, i.e., $|cx_k|^2 \leq P$, and $\boldsymbol{n} \in \mathbb{C}^{2\times 1}$ is an AWGN vector at the dUAV. The transmit power normalization factor c is computed at the dUAV and broadcasted to all of the sUAVs. Later, we elaborate on how the sUAVs obtain the factor c.

Notably, the channels cannot be eliminated at the sUAVs because the sUAVs use a single antenna. In addition, the channel effect cannot be removed from the received signal at the dUAV, as the channels are merged in the air. Accordingly, conventional OAC techniques using multiple transmit antennas, for example, [13], [17], [20], [23], are not directly applicable to sUAVs with a single antenna. In the next section, we propose a novel STLC-OAC strategy for single-antenna sUAVs such that the dUAV can readily estimate the average of the sensing data.

III. PROPOSED STLC-OAC STRATEGY

In this section, a novel STLC-OAC strategy is proposed. We introduce the STLC-based transmission and then elaborate on the protocol for the proposed strategy by discussing how the transmit power normalization factor c in (7) can be obtained for all sUAVs.

A. STLC-BASED TRANSMISSION

In the first phase, the dUAV broadcasts a pilot/traning signal, such that all sUAVs estimate the corresponding channels. Considering a TDD system, the channel from the dUAV to the sUAV and that from the sUAV to the dUAV are assumed to be symmetric. Using the CSI, the kth sUAV generates two STLC symbols $s_{k,1}$ and $s_{k,2}$ from the sensing data x_k as follows:

$$s_{k,1} = h_{k,1}^* x_k + h_{k,2}^* x_k^* = (h_{k,1}^* + h_{k,2}^*) x_k, \tag{8a}$$
$$s_{k,2} = h_{k,2}^* x_k^* - h_{k,1}^* x_k = (h_{k,2}^* - h_{k,1}^*) x_k, \tag{8b}$$

and sequentially transmits them to the dUAV. Notably, $x_k^* = x_k$ as it is a real-valued measurement, and one information data is used to construct the two STLC symbols (i.e., not two information symbols as in the conventional STLC in [28], [29]). After weighting the STLC signals $s_{k,t}$ with $w_{k,t} \in \mathbb{C}^{1\times 1}$ for the OAC at the dUAV and with transmit power normalization factor c, the kth sUAV transmits

$$c w_{k,t} s_{k,t}, \; k \in \mathcal{K} \tag{9}$$

at the tth transmission slot ($t \in \{1, 2\}$). The received signals from all of the sUAVs are then written as follows:

$$y_{1,1} = \sum_{k=1}^{K} h_{k,1} c w_{k,1} s_{k,1} + n_{1,1}, \tag{10a}$$
$$y_{2,1} = \sum_{k=1}^{K} h_{k,2} c w_{k,1} s_{k,1} + n_{2,1}, \tag{10b}$$
$$y_{1,2} = \sum_{k=1}^{K} h_{k,1} c w_{k,2} s_{k,2} + n_{1,2}, \tag{10c}$$
$$y_{2,2} = \sum_{k=1}^{K} h_{k,2} c w_{k,2} s_{k,2} + n_{2,2}, \tag{10d}$$

where $y_{n,t}$ is the signal received by antenna n at time t, and $n_{n,t} \in \mathbb{C}^{1\times 1}$ is the AWGN at $y_{n,t}$. For the STLC, the channels are assumed to be static for two consecutive transmission times, namely $t = 1$ and $t = 2$, yet they may vary in the next STLC transmission for a new sensing data report, i.e., the channel is modeled as a block-fading channel.

The dUAV combines the received signals in (10) to decode the STLC signals as follows:

$$\begin{aligned}
&y_{1,1} + y_{2,2}^* - y_{1,2} + y_{2,1}^* \\
&= c \sum_{k=1}^{K} \left(h_{k,1} w_{k,1} s_{k,1} + h_{k,2}^* w_{k,2}^* s_{k,2}^* \right) \\
&\quad + n_{1,1} + n_{2,2}^* \\
&\quad + c \sum_{k=1}^{K} \left(-h_{k,1} w_{k,2} s_{k,2} + h_{k,2}^* w_{k,1}^* s_{k,1}^* \right) \\
&\quad - n_{1,2} + n_{2,1}^* \\
&= c \sum_{k=1}^{K} w_k \gamma_k x_k + c \sum_{k=1}^{K} w_k^* \gamma_k x_k \\
&\quad + n_{1,1} + n_{2,2}^* - n_{1,2} + n_{2,1}^*,
\end{aligned} \tag{11}$$

where $\gamma_k = |h_{k,1}|^2 + |h_{k,2}|^2$.

By designing the weights $w_{k,t}$ as $w_{k,1} = w_{k,2}^* = w_k = \gamma_k^{-1}$ to eliminate the inter-symbol interferences, the combined STLC signals in (11) can be derived as follows:

$$y_{1,1} + y_{2,2}^* - y_{1,2} + y_{2,1}^* = 2\, c \sum_{k=1}^{K} x_k + n, \tag{12}$$

where $n = n_{1,1} + n_{2,2}^* - n_{1,2} + n_{2,1}^*$. From (12), the dUAV obtains the estimated average of the sensing data as follows:

$$\begin{aligned}
\tilde{\bar{X}}_{STLC} &= \frac{1}{2\, cK} \left(y_{1,1} + y_{2,2}^* - y_{1,2} + y_{2,1}^* \right) \\
&= \frac{1}{K} \sum_{k=1}^{K} x_k + \frac{n}{2cK} \\
&= \bar{X} + \frac{n}{2cK}.
\end{aligned} \tag{13}$$

The NMSE is derived from (13) as follows:

$$\begin{aligned}
\text{NMSE}_{STLC} &= \mathrm{E}\left[\frac{\left| \bar{X} - \tilde{\bar{X}}_{STLC} \right|^2}{|\bar{X}|^2} \right] \\
&= \mathrm{E}\left[\frac{\left| \frac{n}{2cK} \right|^2}{|\bar{X}|^2} \right] \\
&\le \frac{\mathrm{E}\left| \frac{n}{2cK} \right|^2}{\mathrm{E}\,|\bar{X}|^2} = \frac{\sigma_n^2}{c^2 K^2\, \mathrm{E}\,|\bar{X}|^2}.
\end{aligned} \tag{14}$$

B. DESIGN OF TRANSMIT POWER NORMALIZATION FACTOR c

As shown in (9), all sUAVs must know the transmit power normalization factor c to encode the STLC symbols. In addition, to estimate the average value of the sensing data, as shown in (13), the dUAV must know the transmit power normalization factor c and number of sUAVs, i.e., K. It is assumed that the number of sUAVs is predetermined and at the dUAV. However, the transmit power normalization factor c is difficult to be determine at both the sUAVs and dUAV because it depends on the transmit symbol $\{s_{k,t}\}$ of all the sUAVs, namely the channel state information $h_{k,n}$ and sensing data x_k. To resolve this implementation issue, we propose a strategy for designing and sharing c with the dUAV and sUAVs.

Because the transmit power of each sUAV is limited by P, that is $|c w_{k,t} s_{k,t}|^2 \le P$ in (9), the following inequality should

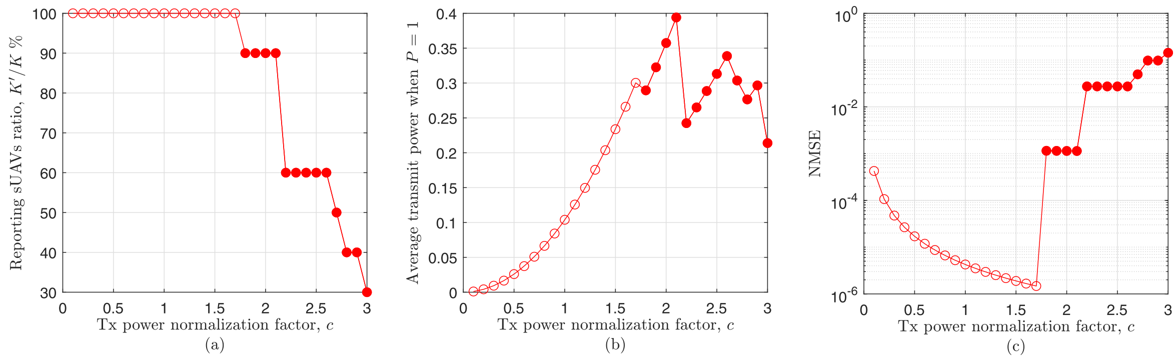

FIGURE 3. Numerical results (one snapshot) over the transmit (Tx) power normalization factor c for the OAC when $K = 10$, $\sigma_v^2 = 0.01$, $N = 4$, $M = 2$, and $P/\sigma_n^2 = 15$ dB. Here, the ground truth measurement value is set as $x^o = 0.3$. (a) Ratio of the number of reporting sUAVs K' over total number of sUAVs K. (b) Transmit power of sUAV when $P = 1$. (c) NMSE.

be satisfied:

$$c \leq \sqrt{\frac{P}{|w_k|^2|s_{k,t}|^2}}, \quad t \in \{1, 2\}. \tag{15}$$

Here, if c is too large, the constraint in (15) becomes too stringent, such that the number of sUAVs fulfilling (15) decreases and number of reporting sUAVs decreases; this is shown in Fig. 3(a), where a reporting sUAV ratio K'/K is evaluated across c. Here, K' is the number of sUAVs fulfilling (15) and reporting the sensing data, whereas the $(K - K')$ sUAVs do not fulfill (15) and do not report. In addition, the transmit power of each sUAV increases as c increases, as shown in Fig. 3(b). The reduction in the number of reporting sUAVs reduces the fidelity of the estimation even with the greater transmit power of each reporting sUAV, resulting in an increase in the NMSE. This can be observed when $c > 1.7$, as shown in Fig. 3(c). If c is too small, the number of reporting sUAVs increases as observed in Fig. 3(a); however, the transmit power of each sUAV is severely suppressed, as observed in Fig. 3(b), resulting in a poor estimation performance, as observed in Fig. 3(c). As observed in Fig. 3, the optimal transmit power normalization factor c^o activates all sUAVs to report the sensing data and should also be as large as possible to increase the transmit power of the sUAVs. Therefore, the optimal transmit power normalization factor c^o is designed as follows:

$$c^o = \min_{k \in \mathcal{K}} b_k, \tag{16}$$

where b_k is the upper bound of the transmit power normalization factor of sUAV k that is defined from (15) as

$$\begin{aligned} b_k &\triangleq \min_{t \in \{1,2\}} \sqrt{\frac{P}{|w_k|^2|s_{k,t}|^2}} \\ &= \min\left\{\frac{\gamma_k\sqrt{P}}{|s_{k,1}|}, \frac{\gamma_k\sqrt{P}}{|s_{k,2}|}\right\} \\ &= \min\left\{\frac{\left(|h_{k,1}|^2 + |h_{k,2}|^2\right)\sqrt{P}}{|(h_{k,1}^* + h_{k,2}^*)x_k|}, \frac{\left(|h_{k,1}|^2 + |h_{k,2}|^2\right)\sqrt{P}}{|(h_{k,2}^* - h_{k,1}^*)x_k|}\right\}. \end{aligned} \tag{17}$$

C. SIGNALING SCENARIO TO OBTAIN TRANSMIT POWER NORMALIZATION FACTOR c

Now, we introduce the scenario for obtaining c^o in (16) for both the dUAV and sUAVs. In the first time slot, the dUAV broadcasts a pilot signal p using the first antenna, and sUAV k estimates $h_{k,1}$. In the second time slot, the dUAV broadcasts a pilot signal p using the second antenna, and sUAV k estimates $h_{k,2}$. Accordingly, sUAV k has its own channel state information, i.e., $\{h_{k,1}, h_{k,2}\}$, and can compute b_k in (17). All sUAVs then report b_k to the dUAV sequentially in orthogonal time slots. The dUAV then determines the optimal transmit power normalization factor based on (16) and broadcasts it to all sUAVs. All sUAVs then generate the STLC signals as in (8), normalize them as in (9), and report the sensing data by using the STLC simultaneously. Therefore, one cycle of the data report of the STLC-based OAC method requires the following transmission time:

$$t_{STLC} = K + 5, \tag{18}$$

where two slots are for training, K slots are for reporting b_k, one slot is for broadcasting c^o, and two slots are for reporting via the STLC scheme in (9). Comparing (18) and (6), it should be emphasized that the proposed STLC-based OAC method requires fewer time slots relative to that of the TDMA-based method if there are more than four sUAVs, that is, if $K > 5$.

For an example of the proposed STLC-OAC strategy, eight slots are required for one cycle of data report from three sUAVs as illustrated in Fig. 4, and the general procedure of the STLC-OAC from the sUAVs is summarized in Algorithm 1.

IV. PERFORMANCE COMPARISON AND DISCUSSION

A. UAV OPERATION TIME

Fig. 5 shows the number of required time slots for one cycle of data report in a TDMA-based strategy, that is, (6), as compared to that in an STLC-OAC strategy, that is, (18). Here, the number of information symbols for the TDMA-based strategy, i.e., $\lceil \frac{N}{M} \rceil$, varies from 1 to 12 according to the

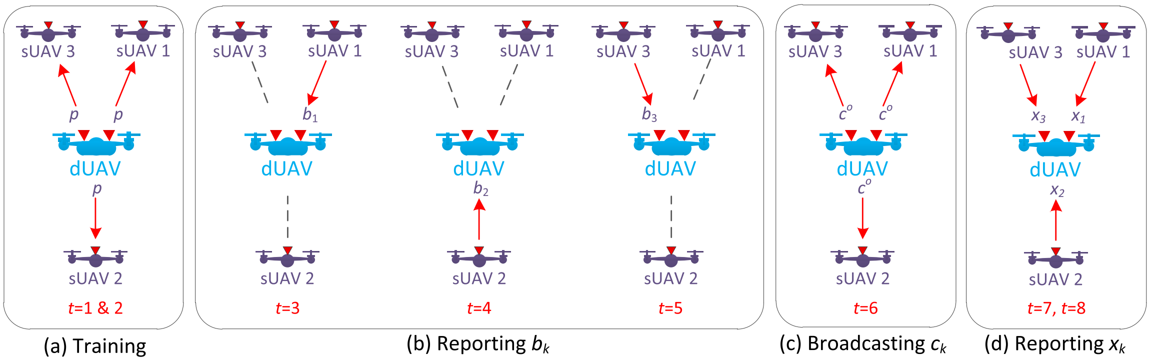

FIGURE 4. Proposed STLC-based OAC method, in which one dUAV computes the average value of the sensing data from three sUAVs. (a) Training for CSI estimation at sUAVs. (b) Reporting the bound of transmit power normalization factor b_k in (17). (c) Broadcasting the transmit power normalization factor c^o in (16). (d) Reporting data based on STLC-OAC strategy.

Algorithm 1 Proposed STLC-Based OAC Method

1: $t = 1$: dUAV sends a pilot signal through the first antenna and all sUAVs estimate $h_{k,1}$.
2: $t = 2$: dUAV sends a pilot signal through the second antenna and all sUAVs estimate $h_{k,2}$.
3: **for** $t = 3$ **to** $K + 2$ **do**
4: The kth sUAV computes and reports b_k to dUAV at time slot t, where $k = t - 2$.
5: **end for**
6: $t = K + 3$: dUAV computes and broadcasts c^o to all sUAVs.
7: $t = K + 4$: All sUAVs reports data simultaneously by using the first STLC symbol transmission in (9), and the dUAV receives $y_{1,1}$ and $y_{2,1}$.
8: $t = K + 5$: All sUAVs reports data simultaneously by using the second STLC symbol transmission in (9), and the dUAV receives $y_{1,2}$ and $y_{2,2}$ and estimates $\tilde{\overline{X}}$ From (13).

number of bits for quantization N and modulation size M. As shown in the results, the number of required time slots increases as the number of sUAVs increases. Even though the TDMA-based strategy transmits one information symbol, i.e., $\lceil \frac{N}{M} \rceil = 1$, the required number of time slots for the TDMA-based strategy is much greater than that of the proposed STLC-OAC strategy, especially when there are many sUAVs, i.e., when K is large. From the results, it is evident that the proposed STLC-OAC can prolong the UAV operation time, and thereby expand the UAV-related business for data collection.

B. COMMUNICATION PERFORMANCE

In this section, the numerical results obtained with various simulation parameters are presented and discussed. Here, the system signal-to-noise ratio (SNR) is defined as P/σ_n^2 *dB*. For the TDMA-based strategy, a uniform quantizer between -1 and 1 was used to digitize the sensing data. For the proposed STLC-OAC strategy, the transmit power normalization factor c was obtained following the scenario

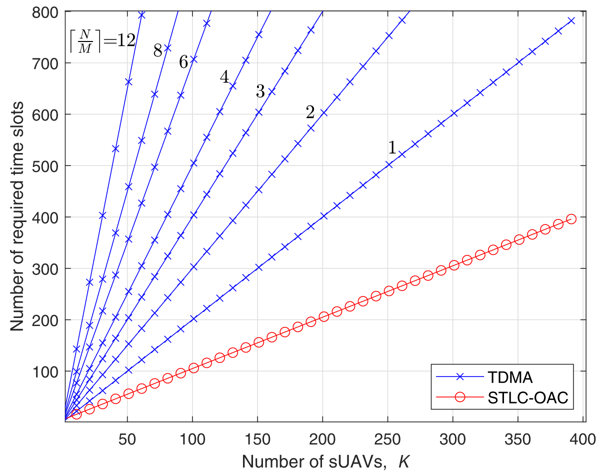

FIGURE 5. Comparison of the numbers of the required time slots for one cycle of data report over the number of sUAVs, K, from 2 to 382.

described in Section III-C. The simulation was performed for different values of ground truth sensing data $x^o \in \{0.1, 0.2, 0.3, 0.4, 0.5, 0.6, 0.7, 0.8, 0.9\}$, and the results are shown in nine subfigures from (a) to (i).

In Fig. 6, the NMSEs of the TDMA-based strategy and proposed STLC-OAC strategy are compared across the system SNR when ten sUAVs (i.e., $K = 10$) report the sensing data to the dUAV. For the TDMA-based strategy, a four-bit uniform quantizer between -1 and 1 was used to digitize the sensing data (as mentioned above), and quadrature phase-shift keying modulation was employed, namely, $N = 4$ and $M = 2$. The sensing error variance was assumed as $\sigma_v^2 = 0.01$. From these results, it is evident that the NMSE decreases as the SNR increases. In particular, in the low SNR regime, the proposed STLC-OAC strategy outperforms the TDMA-based strategy. In general, the proposed STLC-OAC strategy can achieve an NMSE performance comparable to that of the TDMA-based strategy. It should be reemphasized that the required number of time slots for the proposed STLC-OAC strategy is $K + 5 = 15$, whereas that of the TDMA-based strategy is $K \left(\lceil \frac{N}{M} \rceil + 1 \right) = 30$. Thus, considering the energy consumption of the dUAV and sUAVs, it can be surmised

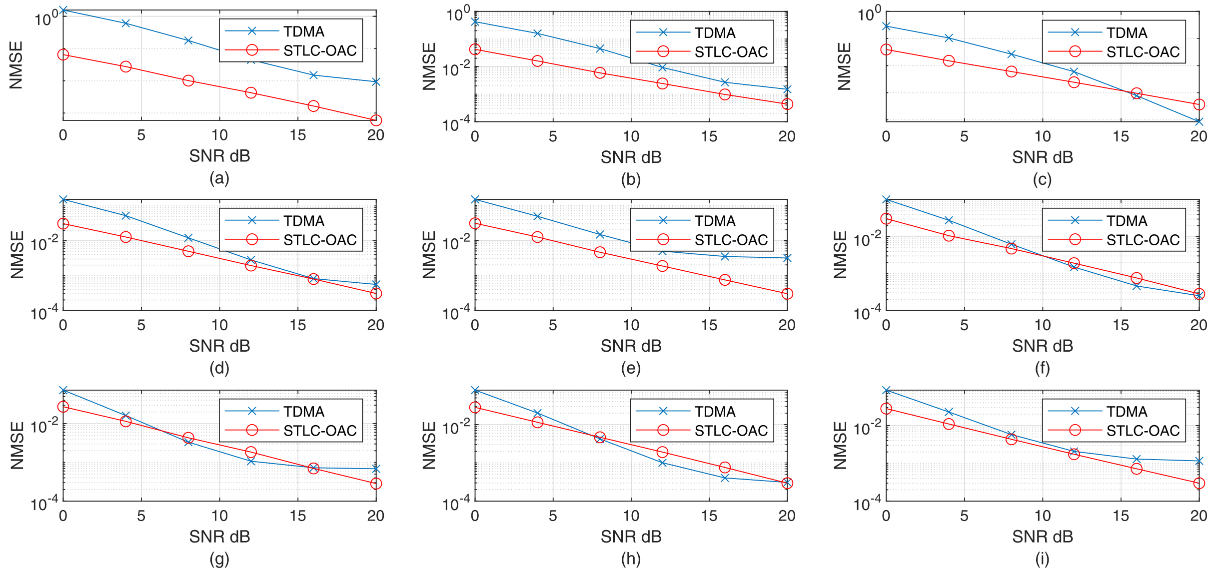

FIGURE 6. NMSE comparison between TDMA-based strategy and proposed STLC-OAC strategy when computing the average value of the sensing data from multiple sUAVs over the SNRs, when $K = 10$, $\sigma_v^2 = 0.01$, $N = 4$, and $M = 2$. (a) $x^o = 0.1$. (b) $x^o = 0.2$. (c) $x^o = 0.3$. (d) $x^o = 0.4$. (e) $x^o = 0.5$. (f) $x^o = 0.6$. (g) $x^o = 0.7$. (h) $x^o = 0.8$. (i) $x^o = 0.9$.

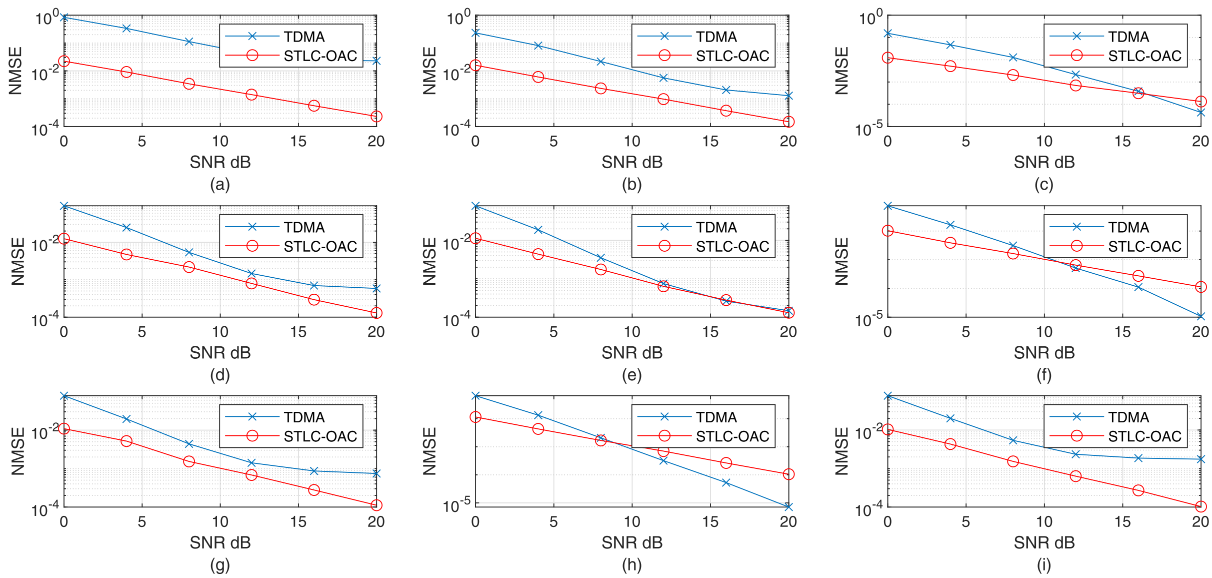

FIGURE 7. NMSE comparison between TDMA-based strategy and the proposed STLC-based OAC strategy when computing the average value of the sensing data from multiple sUAVs over the SNRs, when $K = 10$, $\sigma_v^2 = 0.01$, $N = 4$, and $M = 4$. (a) $x^o = 0.1$. (b) $x^o = 0.2$. (c) $x^o = 0.3$. (d) $x^o = 0.4$. (e) $x^o = 0.5$. (f) $x^o = 0.6$. (g) $x^o = 0.7$. (h) $x^o = 0.8$. (i) $x^o = 0.9$.

that the proposed STLC-OAC strategy is a more effective strategy for dUAVs to collect the sensing data from sUAVs and compute their average values. Moreover, the performance of the TDMA-based strategy highly depends on the design of the quantization and modulation size, namely N and M, and the amount of measurement error, i.e., σ_v^2.

As shown in Fig. 7, to reduce the required time slots for the TDMA-based strategy, the modulation size M can be increased from two to four. As a result, the required number of time slots is reduced from 30 to 20 with the sacrifice of the performance, i.e., the NMSE of the TDMA-based strategy increases. Nevertheless, the number of required time slots is still greater than that of the proposed STLC-OAC strategy. In this case, the proposed STLC-OAC strategy outperforms the TDMA-based strategy in terms of both performance and energy efficiency. Furthermore, the proposed STLC-OAC strategy outperforms the TDMA-based strategy irrespective of the ground truth value, x^o, if the SNR is lower than 10 dB.

In Fig. 8, the NMSEs are evaluated over σ_v^2, i.e., the variance of the sensing data, when the SNR is fixed at 15 dB, $K = 10$, $N = 4$, and $M = 4$ (where $N = M$ is the most energy efficient configuration for the TDMA-based strategy). From the results, it is observed that the NMSE performances of both the TDMA-based and STLC-OAC strategies are almost

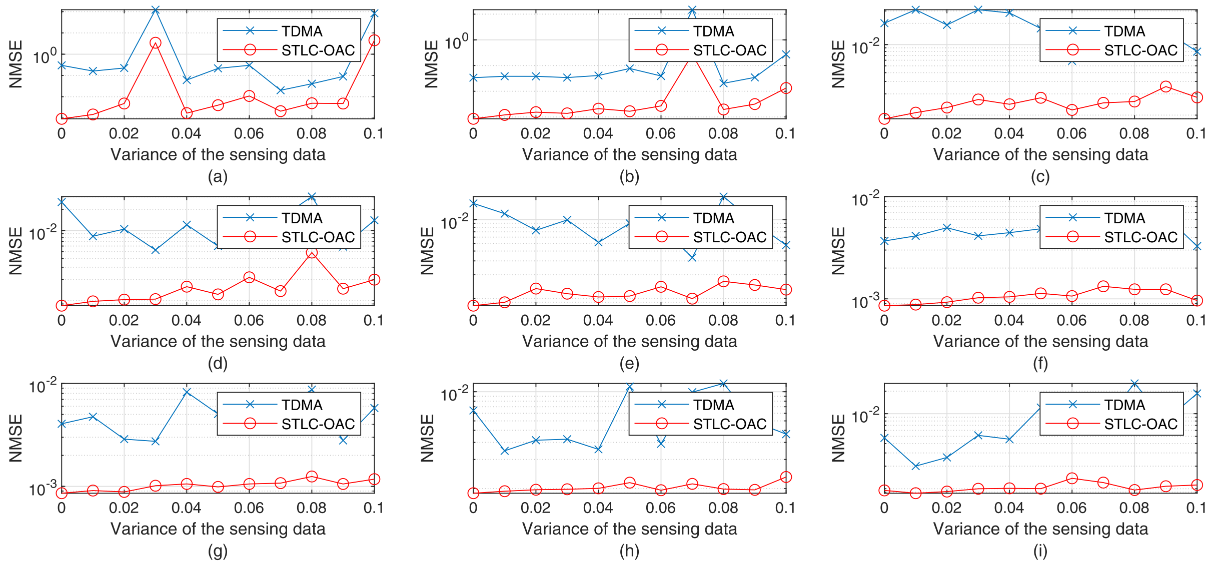

FIGURE 8. NMSE comparison between TDMA-based strategy and proposed STLC-based OAC strategy when computing the average value of the sensing data from multiple sUAVs over the sensing error amount, i.e., σ_v^2, when the SNR is 15 dB, $K = 10$, $N = 4$, and $M = 4$. (a) $x^o = 0.1$. (b) $x^o = 0.2$. (c) $x^o = 0.3$. (d) $x^o = 0.4$. (e) $x^o = 0.5$. (f) $x^o = 0.6$. (g) $x^o = 0.7$. (h) $x^o = 0.8$. (i) $x^o = 0.9$.

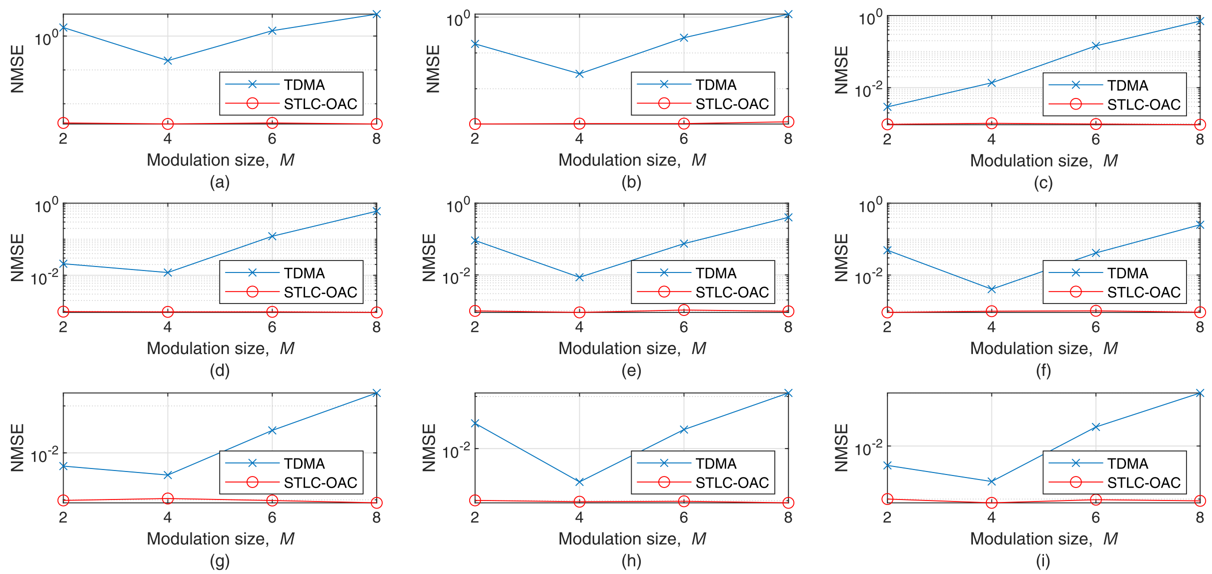

FIGURE 9. NMSE comparison between TDMA-based strategy and the proposed STLC-based OAC strategy when computing the average value of the sensing data from multiple sUAVs over the modulation size M for the TDMA-based method, when the SNR is 15 dB, $\sigma_v^2 = 0.01$, $K = 10$, and $N = M$. (a) $x^o = 0.1$. (b) $x^o = 0.2$. (c) $x^o = 0.3$. (d) $x^o = 0.4$. (e) $x^o = 0.5$. (f) $x^o = 0.6$. (g) $x^o = 0.7$. (h) $x^o = 0.8$. (i) $x^o = 0.9$.

independent of the amount of sensing errors, that is, the variance σ_v^2 of the sensing data. The results, also verify that the proposed STLC-OAC strategy outperforms the TDMA-based strategy irrespective of the sensing error.

In Fig. 9, the NMSEs are evaluated over the modulation size, i.e., M, for the TDMA-based method when the SNR is fixed at 15 dB, $\sigma_v^2 = 0.01$, $K = 10$, and $N = M$. As expected, the performance of the TDMA-based method deteriorates as M increases from four, because the decoding error increases at the dUAV. In most cases, except that shown in Fig. 9(c), the NMSE decreases when M changes from two to four. This is because the benefit obtained from the increase in the quantization resolution (i.e., the increase in N from two to four) is greater than the deterioration caused by the increase in the modulation size. From the results, it is observed that the proposed STLC-OAC strategy outperforms the TDMA-based strategy regardless of the modulation size used for the TDMA-based scheme.

In Fig. 10, the NMSEs are evaluated over the quantization bits, i.e., N, for the TDMA-based strategy when the SNR is fixed at 10 dB, $\sigma_v^2 = 0.01$, $K = 10$, and $M = 2$. As expected, the performance of the TDMA-based strategy improves as N increases, because the quantization error decreases. However,

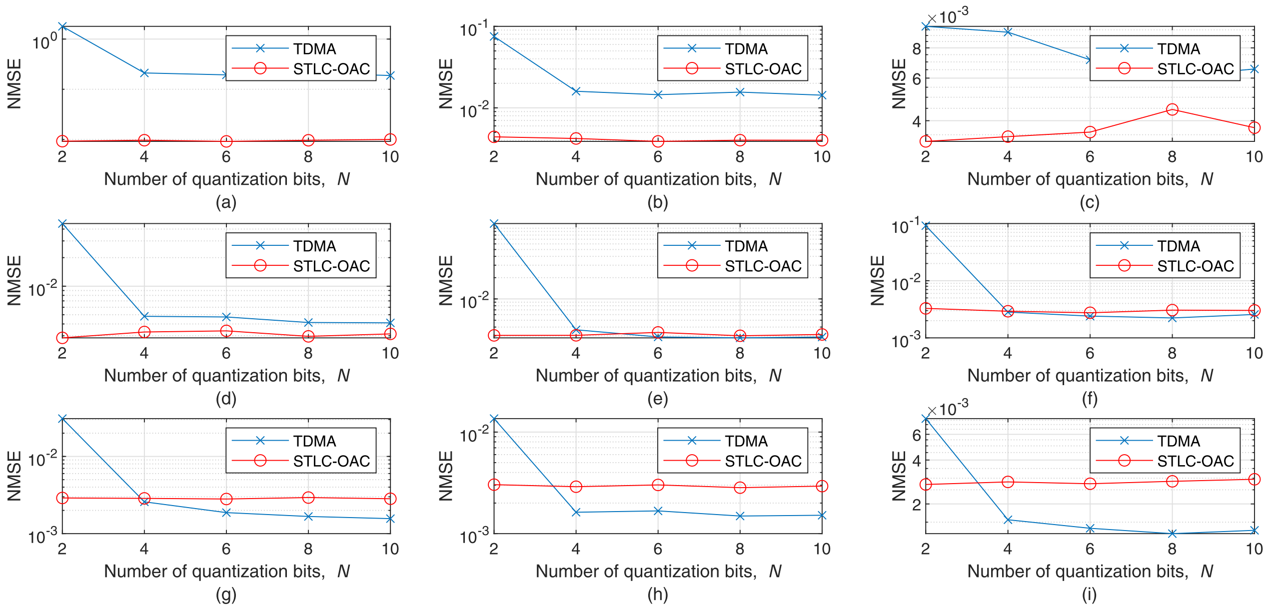

FIGURE 10. NMSE comparison between TDMA-based strategy and proposed STLC-based OAC strategy when computing the average value of the sensing data from multiple sUAVs over the quantization bits N for the TDMA-based method, when the SNR is 10 dB, $\sigma_v^2 = 0.01$, $K = 10$, and $M = 2$. (a) $x^o = 0.1$. (b) $x^o = 0.2$. (c) $x^o = 0.3$. (d) $x^o = 0.4$. (e) $x^o = 0.5$. (f) $x^o = 0.6$. (g) $x^o = 0.7$. (h) $x^o = 0.8$. (i) $x^o = 0.9$.

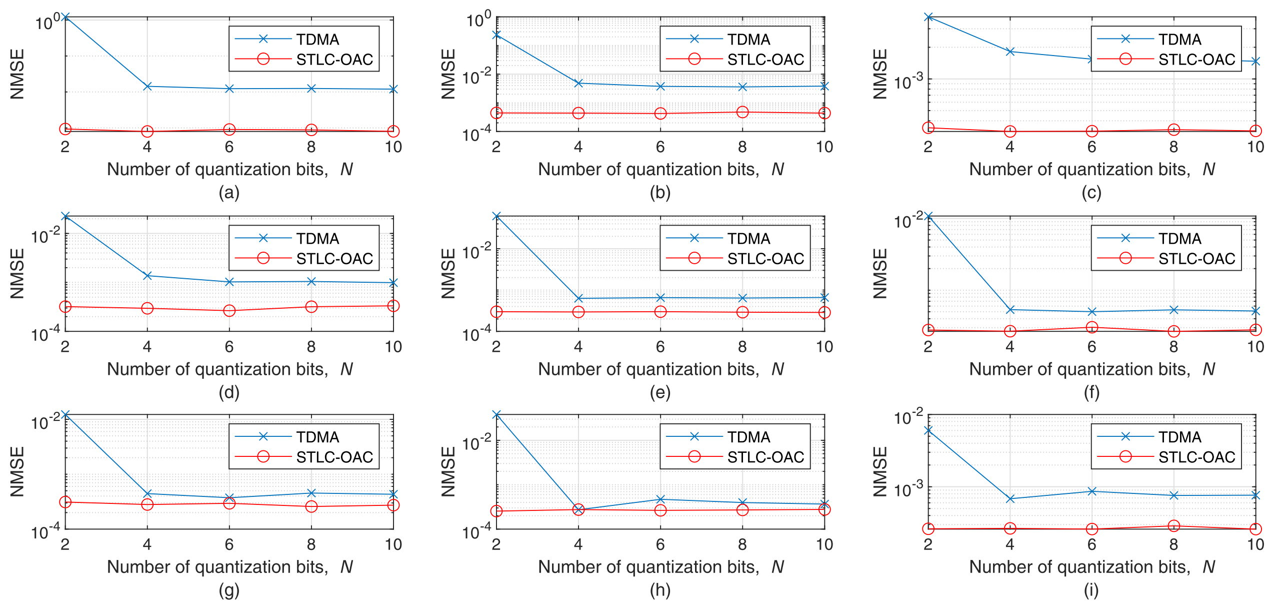

FIGURE 11. NMSE comparison between TDMA-based strategy and proposed STLC-based OAC strategy when computing the average value of the sensing data from multiple sUAVs over the quantization bits N for the TDMA-based method, when the SNR is 10 dB, $\sigma_v^2 = 0.01$, $K = 50$, and $M = 2$. (a) $x^o = 0.1$. (b) $x^o = 0.2$. (c) $x^o = 0.3$. (d) $x^o = 0.4$. (e) $x^o = 0.5$. (f) $x^o = 0.6$. (g) $x^o = 0.7$. (h) $x^o = 0.8$. (i) $x^o = 0.9$.

it should be noted that the required number of time slots for the TDMA-based strategy increases as N increases for at fixed M. This causes a significant increase in the energy consumption of the sUAVs. Furthermore, the results show that the performance of the proposed STLC-OAC strategy is comparable to that of the TDMA-based strategy. However, if there are many sUAVs, that is, if K increases, the proposed STLC-OAC strategy always outperforms the TDMA-based strategy; this can be observed in Fig. 11, where the number of sUAVs is set as $K = 50$.

To clarify the merits of the proposed STLC-OAC strategy, the NMSEs were evaluated over the number of sUAVs, as shown in Fig. 12. In general, the NMSE decreases as the number of sUAVs K increases, as a more accurate estimation is possible by averaging the AWGN. From the results, as expected, the proposed STLC-OAC strategy outperforms the TDMA-based strategy. Overall, it is a good strategy for computing the average value of the sensing data from multiple sUAVs, especially when there are a large number of sUAVs reporting the sensing data.

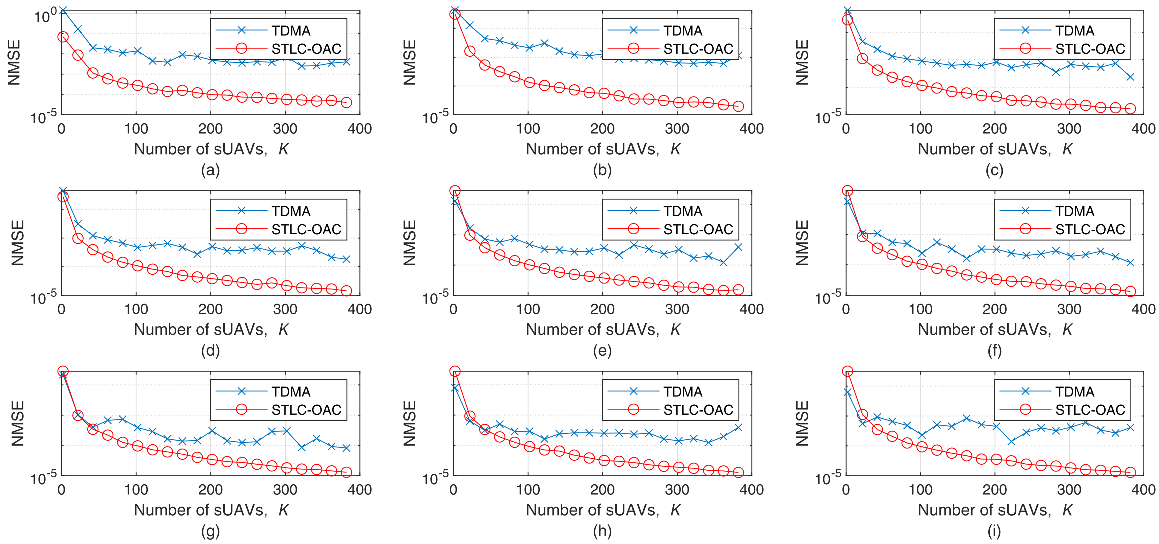

FIGURE 12. NMSE comparison between TDMA-based strategy and proposed STLC-based OAC strategy when computing the average value of the sensing data from multiple sUAVs over the number of sUAVs when the SNR is 10 *dB*, $\sigma_v^2 = 0.01$, $N = 4$, and $M = 2$. (a) $x^o = 0.1$. (b) $x^o = 0.2$. (c) $x^o = 0.3$. (d) $x^o = 0.4$. (e) $x^o = 0.5$. (f) $x^o = 0.6$. (g) $x^o = 0.7$. (h) $x^o = 0.8$. (i) $x^o = 0.9$.

V. CONCLUSION

In this paper, an STLC-based OAC strategy is proposed to efficiently compute the average value of the sensing data from multiple sUAVs. The proposed STLC-OAC strategy can reduce the required time slots for data collection at the dUAV, so that energy-efficient operation can be expected from both dUAVs and sUAVs. Accordingly, an increase in commercial opportunities using UAV-aided data collection can also be expected. Furthermore, the proposed STLC-OAC strategy can improve the estimation performance relative to the conventional TDMA-based data collection strategy. In particular, if there are a large number of sUAVs, the proposed STLC-OAC strategy can provide further performance improvement. Ultimately, it represents an effective potential strategy for data collection from multiple sUAVs.

REFERENCES

[1] K. Miyano, R. Shinkuma, N. B. Mandayam, T. Sato, and E. Oki, "Utility based scheduling for multi-UAV search systems in disaster-hit areas," *IEEE Access*, vol. 7, pp. 26810–26820, 2019.
[2] Q. Hu, C. Wu, Y. Wu, and N. Xiong, "UAV image high fidelity compression algorithm based on generative adversarial networks under complex disaster conditions," *IEEE Access*, vol. 7, pp. 91980–91991, 2019.
[3] C. Wu, B. Ju, Y. Wu, and N. Xiong, "SlimRGBD: A geographic information photography noise reduction system for aerial remote sensing," *IEEE Access*, vol. 8, pp. 15144–15158, 2020.
[4] Y. Jin, Z. Qian, and W. Yang, "UAV cluster-based video surveillance system optimization in heterogeneous communication of smart cities," *IEEE Access*, vol. 8, pp. 55654–55664, 2020.
[5] S. Say, H. Inata, J. Liu, and S. Shimamoto, "Priority-based data gathering framework in UAV-assisted wireless sensor networks," *IEEE Sensors J.*, vol. 16, no. 14, pp. 5785–5794, Jul. 2016.
[6] H.-T. Ye, X. Kang, J. Joung, and Y.-C. Liang, "Optimization for full-duplex rotary-wing UAV-enabled wireless-powered IoT networks," *IEEE Trans. Wireless Commun.*, vol. 19, no. 7, pp. 5057–5072, Jul. 2020.
[7] H.-T. Ye, X. Kang, J. Joung, and Y.-C. Liang, "Optimization for wireless-powered IoT networks enabled by an energy-limited UAV under practical energy consumption model," *IEEE Wireless Commun. Lett.*, vol. 10, no. 3, pp. 567–571, Mar. 2021.
[8] H.-T. Ye, X. Kang, J. Joung, and Y.-C. Liang, "Joint uplink-and-downlink optimization of 3D UAV swarm deployment for wireless-powered IoT networks," *IEEE Internet Things J.*, early access, Mar. 12, 2021, doi: 10.1109/JIOT.2021.3065689.
[9] J. Liu, P. Tong, X. Wang, B. Bai, and H. Dai, "UAV-aided data collection for information freshness in wireless sensor networks," *IEEE Trans. Wireless Commun.*, vol. 20, no. 4, pp. 2368–2382, Apr. 2021.
[10] H. Kang, J. Joung, J. Kim, J. Kang, and Y. S. Cho, "Protect your sky: A survey of counter unmanned aerial vehicle systems," *IEEE Access*, vol. 8, pp. 168671–168710, 2020.
[11] J. Wivou, L. Udawatta, A. Alshehhi, E. Alzaabi, A. Albeloshi, and S. Alfalasi, "Air quality monitoring for sustainable systems via drone based technology," in *Proc. IEEE Int. Conf. Inf. Autom. Sustain. (ICIAfS)*, Galle, Sri Lanka, Dec. 2016, pp. 1–5.
[12] G. M. Bolla, M. Casagrande, A. Comazzetto, R. D. Moro, M. Destro, E. Fantin, G. Colombatti, A. Aboudan, and E. C. Lorenzini, "ARIA: Air pollutants monitoring using UAVs," in *Proc. 5th IEEE Int. Workshop Metrol. Aerosp. (MetroAeroSpace)*, Rome, Italy, Jun. 2018, pp. 225–229.
[13] G. Zhu and K. Huang, "MIMO over-the-air computation for high-mobility multimodal sensing," *IEEE Internet Things J.*, vol. 6, no. 4, pp. 6089–6103, Aug. 2019.
[14] J. Joung, H. Yu, and J. Zhao, "Bandwidth design for energy-efficient unmanned aerial vehicle using space–time line code," *IEEE Syst. J.*, vol. 15, no. 2, pp. 3154–3157, Jun. 2021.
[15] M. Goldenbaum and S. Stanczak, "Robust analog function computation via wireless multiple-access channels," *IEEE Trans. Commun.*, vol. 61, no. 9, pp. 3863–3877, Sep. 2013.
[16] A. Kortke, M. Goldenbaum, and S. Stańczak, "Analog computation over the wireless channel: A proof of concept," in *Proc. IEEE SENSORS*, Valencia, Spain, Nov. 2014, pp. 1224–1227.
[17] S.-W. Jeon and B. C. Jung, "Opportunistic function computation for wireless sensor networks," *IEEE Trans. Wireless Commun.*, vol. 15, no. 6, pp. 4045–4059, Jun. 2016.
[18] O. Abari, H. Rahul, and D. Katabi, "Over-the-air function computation in sensor networks," 2016, *arXiv:1612.02307*. [Online]. Available: http://arxiv.org/abs/1612.02307
[19] L. Chen, N. Zhao, Y. Chen, F. R. Yu, and G. Wei, "Over-the-air computation for IoT networks: Computing multiple functions with antenna arrays," *IEEE Internet Things J.*, vol. 5, no. 6, pp. 5296–5306, Dec. 2018.
[20] S.-W. Jeon and B. C. Jung, "Adaptive analog function computation via fading multiple-access channels," *IEEE Commun. Lett.*, vol. 22, no. 1, pp. 213–216, Jan. 2018.
[21] X. Cao, G. Zhu, J. Xu, and K. Huang, "Optimized power control for over-the-air computation in fading channels," *IEEE Trans. Wireless Commun.*, vol. 19, no. 11, pp. 7498–7513, Nov. 2020.

[22] S. T. Basaran, G. K. Kurt, and P. Chatzimisios, "Energy-efficient over-the-air computation scheme for densely deployed IoT networks," *IEEE Trans. Ind. Informat.*, vol. 16, no. 5, pp. 3558–3565, May 2020.

[23] Y.-S. Lee, K.-H. Lee, and B. C. Jung, "Beamforming techniques for over-the-air computation in MIMO IoT network," *Sensors*, vol. 21, no. 20, pp. 1–14, Nov. 2020.

[24] M. Fu, Y. Zhou, Y. Shi, T. Wang, and W. Chen, "UAV-assisted over-the-air computation," 2021, *arXiv:2101.09856*. [Online]. Available: http://arxiv.org/abs/2101.09856

[25] M. Hua, Y. Wang, M. Lin, C. Li, Y. Huang, and L. Yang, "Joint CoMP transmission for UAV-aided cognitive satellite terrestrial networks," *IEEE Access*, vol. 7, pp. 14959–14968, Jan. 2019.

[26] S. Mirbolouk, M. A. Choukali, M. Valizadeh, and M. C. Amirani, "Relay selection for CoMP-NOMA transmission in satellite and UAV cooperative networks," in *Proc. 28th Iranian Conf. Electr. Eng. (ICEE)*, Tabriz, Iran, Aug. 2020, pp. 1–5.

[27] Y. Zeng, R. Zhang, and T. J. Lim, "Wireless communications with unmanned aerial vehicles: Opportunities and challenges," *IEEE Commun. Mag.*, vol. 54, no. 5, pp. 36–42, May 2016.

[28] J. Joung, "Space–time line code," *IEEE Access*, vol. 6, pp. 1023–1041, Feb. 2018.

[29] J. Joung, "Space–time line code for massive MIMO and multiuser systems with antenna allocation," *IEEE Access*, vol. 6, pp. 962–979, Feb. 2018.

[30] J. Joung and J. Choi, "Uneven power amplifier shuffling for space-time line code (STLC) systems," *IEEE Access*, vol. 6, pp. 58491–58500, Oct. 2018.

[31] J. Joung and B. C. Jung, "Machine learning based blind decoding for space–time line code (STLC) systems," *IEEE Trans. Veh. Technol.*, vol. 68, no. 5, pp. 5154–5158, May 2019.

[32] J. Joung and E.-R. Jeong, "Multiuser space–time line code with optimal and suboptimal power allocation methods," *IEEE Access*, vol. 6, pp. 51766–51775, Oct. 2018.

[33] J.-B. Seo, H. Jin, J. Joung, and B. C. Jung, "Uplink NOMA random access systems with space–time line code," *IEEE Trans. Veh. Technol.*, vol. 69, no. 4, pp. 4522–4526, Apr. 2020.

[34] J. Joung, "Random space–time line code with proportional fairness scheduling," *IEEE Access*, vol. 8, pp. 35253–35262, Feb. 2020.

[35] J. Joung, J. Choi, and B. C. Jung, "Double space–time line codes," *IEEE Trans. Veh. Technol.*, vol. 69, no. 2, pp. 2316–2321, Feb. 2020.

[36] J. Joung and J. Choi, "Multiuser space–time line code with transmit antenna selection," *IEEE Access*, vol. 8, pp. 71930–71939, Apr. 2020.

[37] J. Joung, "Energy efficient space–time line coded regenerative two-way relay under per-antenna power constraints," *IEEE Access*, vol. 6, pp. 47026–47035, Sep. 2018.

[38] J. Joung and J. Choi, "Space–time line codes with power allocation for regenerative two-way relay systems," *IEEE Trans. Veh. Technol.*, vol. 68, no. 5, pp. 4884–4893, May 2019.

[39] J. Joung, B. C. Jung, and J. Choi, "Space–time line coded regenerative two-way relay systems with power control," *IET Electron. Lett.*, vol. 55, no. 12, pp. 694–696, Jun. 2019.

[40] C. Wu, Y. Xiao, Y. L. Guan, J. Wang, X. Li, and P. Yang, "Space-time/frequency line coded OFDM: System design and practical implementation," *IEEE Access*, vol. 7, pp. 151915–151928, Oct. 2019.

[41] H. Yu and J. Joung, "Frame structure design for vehicular-to-roadside unit communications using space–time line code under time-varying channels," *IEEE Syst. J.*, vol. 15, no. 2, pp. 3150–3153, Jun. 2021.

[42] J. Joung, J. Choi, B. C. Jung, and S. Yu, "Artificial noise injection and its power loading methods for secure space–time line coded systems," *Entropy*, vol. 21, no. 5, pp. 1–12, May 2019.

[43] J. Choi, J. Joung, and B. C. Jung, "Space–time line code for enhancing physical layer security of multiuser MIMO uplink transmission," *IEEE Syst. J.*, early access, Jun. 26, 2020, doi: 10.1109/JSYST.2020.3001068.

[44] Y. Pang, Y. Xiao, X. Lei, and Y. Li, "Performance analysis and antenna selection for space time line code," *IEEE Access*, vol. 8, pp. 193503–193511, Oct. 2020.

[45] S.-C. Lim and J. Joung, "Transmit antenna selection for space–time line code systems," *IEEE Trans. Commun.*, vol. 69, no. 2, pp. 786–798, Feb. 2021.

[46] S. Kim, "Efficient transmit antenna subset selection for multiuser space–time line code systems," *Sensors*, vol. 21, no. 8, pp. 1–21, Apr. 2021.

JINGON JOUNG (Senior Member, IEEE) received the B.S. degree in radio communication engineering from Yonsei University, Seoul, South Korea, in 2001, and the M.S. and Ph.D. degrees in electrical engineering and computer science from KAIST, Daejeon, South Korea, in 2003 and 2007, respectively.

He was a Postdoctoral Fellow with KAIST and UCLA, CA, USA, in 2007 and 2008, respectively. He was a Scientist with the Institute for Infocomm Research (I^2R), Agency for Science, Technology and Research (A*STAR), Singapore, from 2009 to 2015, and joined Chung-Ang University (CAU), Seoul, in 2016, as a Faculty Member. He is currently an Associate Professor with the School of Electrical and Electronics Engineering, CAU, where he is also the Principal Investigator of the Intelligent Wireless Systems Laboratory. His research interests include wireless communication signal processing, numerical analysis, algorithms, and machine learning.

Dr. Joung was a recipient of the First Prize of the Intel-ITRC Student Paper Contest, in 2006. He was recognized as the Exemplary Reviewer of the IEEE COMMUNICATIONS LETTERS, in 2012, and the IEEE WIRELESS COMMUNICATIONS LETTERS, in 2012, 2013, 2014, and 2019. He served as an Editorial Board Member for the *APSIPA Transactions on Signal and Information Processing*, from 2014 to 2019; a Guest Editor for IEEE ACCESS, in 2016, and the *Electronics*, in 2019; and an Associate Editor for the *Sensors*, in 2020. He has been serving as an Associate Editor for the IEEE TRANSACTIONS ON VEHICULAR TECHNOLOGY, since 2018. He is also an Inventor of a Space–Time Line Code (STLC) that is a fully symmetric scheme to a Space–Time Block Code also known as Alamouti code.

JIANCUN FAN (Senior Member, IEEE) received the B.S. and Ph.D. degrees in electrical engineering from Xi'an Jiaotong University, Xi'an, Shaanxi, China, in 2004 and 2012, respectively. From August 2009 to August 2011, he was a Visiting Scholar with the School of Electrical and Computer Engineering, Georgia Institute of Technology, Atlanta, GA, USA. From September 2017 to December 2017, he was a Visiting Scholar with the Technische Universität Dresden (TUD), Germany. He is currently an Associate Professor and the Associate Dean of the School of Information and Communications Engineering, Xi'an Jiaotong University. His general research interests include signal processing and wireless communications, with emphasis on MIMO communication systems, cross-layer optimization for spectral- and energy-efficient networks, practical issues in 5G and 6G systems, and machine learning application for wireless communication. In these areas, he has published over 60 journals and conference papers. He was a recipient of the Best Paper Award at the 20th International Symposium on Wireless Personal Multimedia Communications, in 2017.